RESEARCH ARTICLE

NANO · MICRO small
www.small-journal.com

Lab-in-a-Vial Rapid Test for Internet of Things-Embedded Point-of-Healthcare Protein Biomarker Detection in Bodily Fluids

*Nan-Si Li, Ying-Pei Hsu, Hao-Han Pang, Sheng-Fan Wang, See-Tong Pang, Chih-Yen Lin, Rung-Ywan Tsai, Chiung-Yin Huang, Kuo-Chen Wei, and Hung-Wei Yang**

Amateurs often struggle with detecting and quantifying protein biomarkers in body fluids due to the high expertise required. This study introduces a Lab-in-a-Vial (LV) rapid diagnostic platform, featuring hydrangea-like platinum nanozymes (PtNH), for rapid, accurate detection and quantification of protein biomarkers on-site within 15 min. This method significantly enhances detection sensitivity for various biomarkers in body fluids, surpassing traditional methods such as enzyme-linked immunosorbent assays (ELISA) and lateral flow assays (LFA) by ≈250 to 1300 times. The LV platform uses a glass vial coated with specific bioreceptors such as antigens or antibodies, enabling rapid in vitro evaluation of disease risk from small fluid samples, similar to a personal ELISA-like point-of-care test (POCT). It overcomes challenges in on-site biomarker detection, allowing both detection and quantification through a portable wireless spectrometer for healthcare internet of things (H-IoT). The platform's effectiveness and adaptability are confirmed using IgG/IgM antibodies from SARS-CoV-2 infected patients and nuclear matrix protein (NMP22) from urothelial carcinoma (UC) patients as biomarkers. These tests demonstrated its accuracy and flexibility. This approach offers vast potential for diverse disease applications, provided that the relevant protein biomarkers in bodily fluids are identified.

1. Introduction

In the current dynamic healthcare landscape, there's an urgent need for rapid, accurate diagnostic tools, underscored by challenges like global pandemics and diseases such as cancer. Accurate diagnoses are crucial for timely treatment and limiting infectious disease spread. Traditional diagnostic methods, though reliable, lack speed and convenience, a shortcoming highlighted during events like the COVID-19 pandemic. Moreover, conditions like cancer necessitate sensitive, user-friendly tools, given that existing systems can be cumbersome, invasive, and cause diagnostic delays. The intrinsic value of our work lies in nurturing advancements that strengthen the fields of biomarker-centric diagnostics, vital for addressing conditions such as cancer and various infectious diseases.

For instance, COVID-19 has persistently afflicted the world, resulting in a severe

N.-S. Li, H.-H. Pang, H.-W. Yang
Department of Biomedical Engineering
National Cheng Kung University
Tainan 70101, Taiwan
E-mail: howardyang@gs.ncku.edu.tw

Y.-P. Hsu
Department of Materials and Optoelectronic Science
National Sun Yat-sen University
Kaohsiung 80424, Taiwan

S.-F. Wang, C.-Y. Lin
Department of Medical Laboratory Science and Biotechnology
Kaohsiung Medical University
Kaohsiung 80708, Taiwan

S.-F. Wang
Center for Tropical Medicine and Infectious Diseases Research
Kaohsiung Medical University
Kaohsiung 80708, Taiwan

S.-T. Pang
Division of Urology
Department of Surgery
Chang Gung Memorial Hospital Linkou
Taoyuan 33305, Taiwan

The ORCID identification number(s) for the author(s) of this article can be found under https://doi.org/10.1002/smll.202400878

S.-T. Pang, K.-C. Wei
Department of Medicine
College of Medicine
Chang Gung University
Taoyuan 33302, Taiwan

R.-Y. Tsai
Caduceus Biotechnology Inc.
Hsinchu 302041, Taiwan

C.-Y. Huang, K.-C. Wei
Department of Neurosurgery
Neuroscience Research Center
Chang Gung Memorial Hospital Linkou
Taoyuan 33305, Taiwan

C.-Y. Huang, K.-C. Wei
Department of Neurosurgery
New Taipei Municipal TuCheng Hospital
Taoyuan 23652, Taiwan

H.-W. Yang
Medical Device Innovation Center
National Cheng Kung University
No. 1, University Rd., Tainan City 70101, Taiwan

DOI: 10.1002/smll.202400878

pandemic. Although vaccines have now been developed to prevent severe infections, the ongoing need for robust screening technologies to detect COVID-19 remains crucial in the face of established diseases caused by SARS-CoV-2, its mutant variants, or any emerging infectious pathogens. Moreover, a significant proportion—estimated at 30% to 40%—of COVID-19 infections exhibit asymptomatic characteristics within a 14-day period, with 40% of transmissions occurring before symptom onset.[1] Asymptomatic cases serve as reservoirs and play a pivotal role in the community spread of the virus.

In the realm of COVID-19 diagnostics, RT-qPCR nucleic acid molecular diagnostic tests are primarily utilized to clinically ascertain a positive infection diagnosis. Despite their high accuracy, the costs associated with these tests remain relatively elevated. Current testing protocols necessitate that samples be sent to a certified central laboratory (at a minimum of biosafety level 3) for analysis. Regrettably, the screening duration, which is at least 4 h, cannot be reduced owing to the procedural mandates of central laboratories.[2] Moreover, the employment of this test for frontline point-of-care screening is impractical due to the requirements for specialized equipment, highly trained personnel, and intricate initial sample processing. Considering the formidable challenges outlined above, this approach has been deemed inadequate as a rapid screening tool.

Consequently, the most promising candidates for effective testing are antigen-based and antibody-based methods. An illustrative example of an antigen rapid test is the lateral flow assay (LFA), which delivers rapid results with notable specificity. However, these tests still require nasopharyngeal swabs and demonstrate diminished sensitivity in cases of low viral load. Recent studies on rapid SARS-CoV-2 antigen tests have shown considerable variability in sensitivity, ranging from 0% to 94%, with an average sensitivity of 56.2% (95% CI: 29.5–79.8%).[3] A nationwide systematic evaluation of sensitivity and specificity in mass testing using rapid SARS-CoV-2 antigen lateral flow tests revealed that optimal performance is achieved when tests are conducted by laboratory scientists (78.8%, 95% CI: 72.4–84.3%), compared to self-trained members of the public following a protocol (57.5%, 95% CI: 52.3–62.6%; $p < 0.0001$).[4] Essentially, the accuracy of the antigen LFA depends significantly on the expertise of the test operator.

Furthermore, the COVID-19 pandemic has profoundly impacted healthcare systems globally. In the context of urothelial carcinoma (UC), many patients face delays of at least 6 weeks before receiving a cystoscopy. Such delays carry significant repercussions for the monitoring of both newly diagnosed and recurrent UC.[5] Given this backdrop, there has been a push toward identifying cost-effective and non-invasive alternatives to cystoscopy. The challenge of delivering cancer care during the ongoing pandemic is heightened by the dual risks of cancer-specific mortality and a potentially fatal COVID-19 infection. Currently, Nuclear Matrix Protein 22 (NMP22) has emerged as a crucial urine biomarker for the diagnosis and continued surveillance of urothelial carcinoma (UC).[6,7] As a non-invasive diagnostic marker detectable in urine, NMP22 presents clear advantages, especially when contrasted with the invasive and often uncomfortable traditional cystoscopy procedures. By monitoring NMP22 levels in urine consistently, medical professionals can chart the progression of UC and assess therapeutic efficacy, promoting more tailored and effective treatment regimens. Such monitoring has the potential to significantly improve patient prognosis and their quality of life. This scenario underscores the pressing need for a point-of-care test (POCT) tailored for the efficient management of UC, particularly in these pandemic times.

Enzyme-linked immunosorbent assays (ELISA) and lateral flow assays (LFA) are traditionally employed for the detection of proteins, specifically antibodies and antigens. However, the conventional ELISA process is suboptimal for rapid screening due to its lengthy procedures and the requirement for skilled technicians, in addition to its complex steps. Notably, IgM and IgG antibodies are typically undetectable using traditional ELISA methods until 5–7 days after symptom onset. Additionally, ELISA struggles to detect antigens reliably at concentrations below 1 ng mL^{-1}.[8] On the other hand, conventional LFAs frequently do not possess the sensitivity needed to identify early IgM responses (within the initial 7 days post-symptom onset) or trace amounts of antigens in the preliminary stages of cancer.[9,10] In most cases, the detection sensitivity of LFAs lags behind that of ELISA, which might lead to potential false negatives during the early stages of infectious disease detection.[3] Consequently, there is an urgent need to develop a rapid test that boasts high detection sensitivity, exceptional specificity, and is compatible with various specimen types, such as blood, serum, urine, saliva, and tears.

To address the need for portable and rapid biomarker detection, we conceptualized and developed an innovative Lab-in-a-Vial (LV) rapid diagnostic platform. This platform integrates glass vials with hydrangea-like platinum nanozymes (PtNH) to enable rapid protein tests. Designed for ultrasensitivity, it can detect proteins at pg mL^{-1} concentrations across various samples, including blood, serum, urine, saliva, and tear. First, we showcase the Lab-in-a-Vial's capability for ultrasensitive monitoring of immune responses (IgM and IgG antibodies) to SARS-CoV-2. This allows for detection at notably early stages, with remarkable sensitivity for asymptomatic cases and within a day of symptom onset. Second, we present its efficacy in the sensitive, quantitative, and longitudinal tracking of cancer biomarkers (e.g., NMP22) in the urine of UC patients pre- and post-surgery. Last, we verified the precision of a newly designed portable spectrometer (MiniSpec, HC-PS01) from Caduceus Biotechnology Inc. in measuring solution optical density within the vial, which aids in the quantification of target protein concentrations post-analysis. Overall, this LV rapid diagnostic platform emerges as a versatile diagnostic instrument, valuable in combating viral spread, early cancer detection, and managing post-surgical cancer recurrence risk. Its potential is especially profound for enhancing global public healthcare accessibility during challenges such as the COVID-19 pandemic and possible emerging pandemics in the future.

2. Results

2.1. Characterizations of PtNH-Based Signal Probes and Diagnostic Vials

We have proposed an advanced concept of a portable diagnostic laboratory and have engineered the "Lab-in-a-Vial" rapid diagnostic platform (**Figure 1**). This system integrates a high-catalytic PtNH-based signal probe with a tunable diagnostic vial. This platform is not only conducive to the rapid detection of a wide range

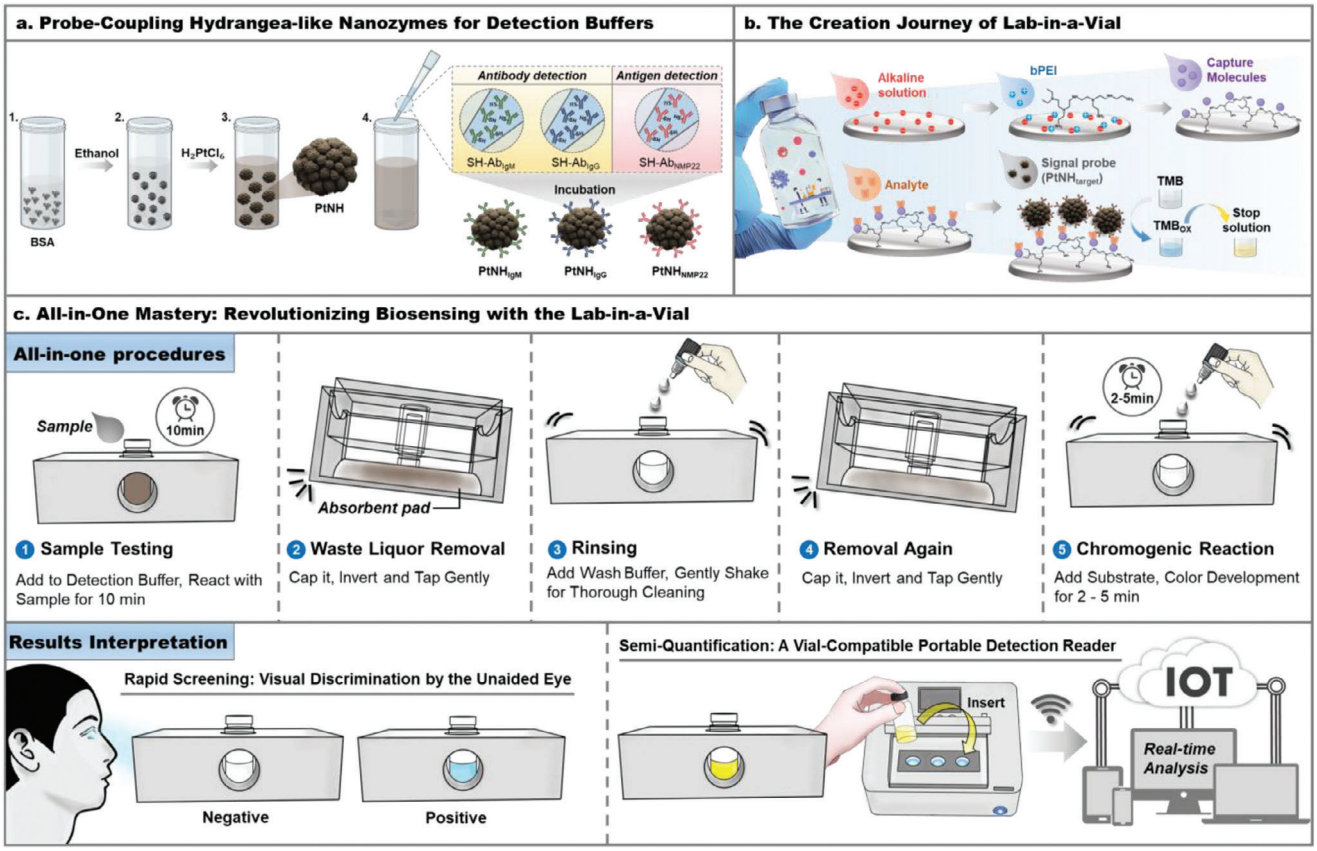

Figure 1. Schematic illustration of the innovative LV rapid diagnostic kit designed for the detection and quantification of point-of-care protein biomarkers in bodily fluids. a) The synthesis of probe-coupling PtNH for detection buffers, b) The journey and mechanism involved in creating the LV, c) The all-in-one procedures of LV rapid diagnostic kit.

of protein molecules but is also optimally suited for point-of-care health applications.

For PtNH-based signal probe fabrication, we prepared PtNH with a mean size of 51.8 ± 3.8 nm and a high catalytic surface area as nanozymes. To gain a deeper understanding of the distribution of Pt in PtNH, we conducted elemental analysis on the PtNH using energy-dispersive X-ray spectroscopy (EDS). This analysis yielded a Pt content of ≈55.3%, with the remaining 44.7% comprising other elements associated with bovine serum albumin (BSA) (25.5% N, 16.2% O, and 3.0% S) within the PtNH (Figure S1a, Supporting Information). This result serves as evidence that the Pt nanoclusters were indeed capped onto the BSA template. The synthesized PtNH exhibited notable peroxidase-mimetic activity, promoting the oxidation of TMB in the presence of H_2O_2, leading to a distinct colorimetric change (Figure S1b, Supporting Information). Further exploration into the enzymatic kinetics of the PtNH showed that the Michaelis–Menten constant, K_m, of the PtNH was 185.02 μM, whereas for free horseradish peroxidase (HRP), K_m was ≈175.20 μM, indicating the similar affinity toward substrate H_2O_2. However, once the substrate reaches the active site of PtNH, the catalytic efficiency is enhanced, resulting in a higher V_{max} (2.69 μM s^{-1}) compared to free HRP (1.73 μM s^{-1}). This increase is attributed to the hydrangea-like structure of PtNH, which provides a larger surface area and more active sites, as well as an optimized microenvironment that reduces product feedback inhibition (Figure S2, Supporting Information).[11,12] The results confirm that PtNH exhibit superior catalytic performance, making them highly suitable as signal probes for diagnostic applications.[13,14]

In terms of stability, PtNH outperformed HRP. This superiority is underscored by the pronounced decrease in HRP's peroxidative activity on the H_2O_2/TMB substrate after treatment with 0.05 wt.% trypsin at 37 °C, while the activity of PtNH remained predominantly consistent (Figure S3a,b, Supporting Information). We further assessed the thermal stability of both HRP and PtNH over storage periods ranging from 1 to 21 days at 25, 37, and 50 °C. As depicted in Figure S3c (Supporting Information), HRP lost its full activity after a mere 3 days stored at 50 °C and failed to retain its activity past 21 days at 25 °C. In contrast, PtNH effectively oxidized H_2O_2/TMB without sensitivity loss when stored at 37 °C for 21 days. Only a reduction of 28.5% from the initial activity was observed after a 21-day storage at 50 °C, a stability that HRP could not match. Moreover, PtNH show a more versatile pH range for oxidizing H_2O_2/TMB compared to HRP. The results demonstrated that HRP's peroxidative activity is pH-sensitive, peaking at pH 6 and tapering off at higher or lower values. Conversely, PtNH maintained consistent peroxidation activity across a broad pH range of 3–11, regardless of pH fluctuations (Figure S3d, Supporting Information). Taking together, these PtNH, with their capacity for ready

functionalization with detection antibodies, emerge as a viable alternative to HRP, enabling the fabrication of highly sensitive signal probes.

Subsequently, the quantities of Ab_{IgG} bound to PtNH were quantified by analyzing the unbound antibodies in the supernatant using an ELISA method. The grafting efficiency of Ab_{IgG} on PtNH (0.5 mL, $OD_{290nm} = 0.5$) exhibited an increase with the addition of higher concentrations of Ab_{IgG} (100, 200, 300, 400, 500, 600, and 700 ng). The resulting grafting efficiencies were 90.04 ± 9.74%, 94.53 ± 4.90%, 96.11 ± 3.34%, 97.12 ± 2.55%, 97.54 ± 2.10%, 97.78 ± 1.89%, and 97.95 ± 1.74%, respectively (Figure S4, Supporting Information). However, considering the limited surface area available for biomolecule capture on the glass vial and the fact that increasing the quantity of antibodies beyond a certain threshold does not significantly improve the detection of low-concentration antigens, the economic impact of biomolecule use in large-scale production of diagnostic kits must be considered. An exponential increase in antibody consumption significantly raises costs. Therefore, we identified 200 ng of antibody per 0.5 mL PtNH ($OD_{290nm} = 0.5$) as the optimal parameter for this study. This amount not only ensures efficient grafting but also meets the required sensitivity for detection.

For diagnostic vial fabrication, we proposed a green and simple manufacturing process to produce rich amine-functionalized vial by deposition of branched polyethyleneimine (bPEI) on an ethanol pretreated vial; then, the specific antigen or antibody was immobilized on the bPEI-modified vial by electrostatic adsorption force. Consequently, we investigated the optimal coating concentration of bPEI for our purposes (Figure S5, Supporting Information). The results demonstrated that a 0.5 wt.% bPEI coating did not yield false-negative background signals within 8 min. In contrast, the 0.75 wt.% bPEI coating began to generate background signals after 5 min. Therefore, to guarantee that the rapid and ultrasensitive LV test can effectively distinguish between positive and negative results via visual inspection, the optimal concentration of bPEI was determined to be 0.5 wt.%. As depicted in Figure S6a (Supporting Information), the successful amine group modification on the vial was confirmed by the TNBS assay; a deeper yellow color and higher absorbance intensity at 345 nm were observed after bPEI coating. Then the successful immobilization of antigen or antibody to form diagnostic vials was confirmed by BCA assay, and higher absorbance intensity at 562 nm was observed when the SARS-CoV-2 N-protein was added in the bPEI-coated vial compared with that in the blank vial (Figure S6b, Supporting Information). Finally, we prepared the signal probes (i.e., $PtNH_{IgG}$, $PtNH_{IgM}$, $PtNH_{NMP22}$) and the diagnostic vials (i.e., $Vial_{COV}$ and $Vial_{UC}$) and evaluated the feasibility of assembling them into a detection platform. As depicted in Figure S6c (Supporting Information), no color change was observed when PtNH/anti-SARS-CoV-2 N-protein IgG or PtNH/anti-SARS-CoV-2 N-protein IgM solution was added to the $Vial_{COV}$. Conversely, a significant blue color was observed when $PtNH_{IgG}$/anti-N-protein IgG or $PtNH_{IgM}$/anti-N-protein IgM solution was added to the $Vial_{COV}$. The aforementioned results demonstrate that we successfully fabricated tunable nanozymes as the signal probes and diagnostic vials, and integrated them to construct LV rapid diagnostic kit that can be broadly employed for the rapid detection of protein-based biomarkers. Therefore, in this study, we will use the detection of COVID-19 and UC as validation to assess the feasibility of this LV rapid diagnostic kit in clinical diagnostics.

2.2. Three Vials-Based LV Rapid Test for Anti-SARS-CoV-2 N-Protein IgM/IgG Antibody Detection

We've developed a cutting-edge rapid diagnostic platform for bodily fluids called LV rapid test, which is highly sensitive and user-friendly. This biosensor is specifically designed for the quick and straightforward detection of protein biomarkers, including both antigens and antibodies, in patients. Herein, we initially explored the potential of this sensor for rapidly testing viral infections, with a specific focus on SARS-CoV-2, the virus responsible for COVID-19. To achieve this, we designed a three vials-based LV ($3LV_{COV}$) rapid diagnostic kit comprises an operation cassette equipped with three $Vial_{COV}$ units and a lid with an adsorbent pad, dropper bottles filled with filled with detection buffer ($PtNH_{IgG}$ solution and $PtNH_{IgM}$ solution), wash buffer (PBS), and a chromogenic substrate (TMB/H_2O_2). For this particular case study, we selected the SARS-CoV-2 N-protein as the capture probe to create $Vial_{COV}$ due to its strong immunogenic response following human infection with SARS-CoV-2.

The assay procedures start with dripping 16 drops of $PtNH_{IgM}$ solution into the two $Vial_{COV}$, which were placed in the left (control) and middle (for IgM antibody detection) slots and $PtNH_{IgG}$ solution into the $Vial_{COV}$ placed in the right (for IgG antibody detection) slot of the cassette, and then transferring 5 µL of fresh serological samples into the middle and right $Vial_{COV}$ via microdropper and followed by gently shaking the cassette for a short while and incubating for 10 min. After that, the three $Vial_{COV}$ were washed by dripping the PBS solution, followed by the introduction of the chromogenic substrate to initiate color development (**Figure 2a**).

In this case study, we utilized the $3LV_{COV}$ rapid diagnostic kit to analyze 163 clinical samples, consisting of 39 positive clinical samples [9 serum samples from Kaohsiung Medical University (KMU), 20 serum samples from National Health Research Institutes (NHRI), and 10 early infection serum samples imported from the United States] and 124 negative clinical samples [10 fingerstick blood samples from healthy volunteers at Chang Gung Memorial Hospital (CGMH), 39 serum samples from KMU (encompassing various upper respiratory infection specimens), 70 serum samples from NHRI (influenza A/B specimens), and 5 serum samples imported from the United States] (**Table 1**). We conducted a statistical analysis of the results by measuring the absorbance intensity at 450 nm (A_{450}) of the Ctrl/IgM/IgG testing vials for the 163 clinical samples using a spectrophotometer. The scatter interval plot revealed that all A_{450} values for Ctrl/IgM/IgG testing vials corresponding to healthy subjects (denoted in white), individuals with upper respiratory tract infections or prior influenza A/B infections (denoted in blue) were below the threshold of 0.015. In contrast, nearly all A_{450} values for IgM/IgG testing vials corresponding to patients confirmed to be infected with SARS-CoV-2 by PCR were greater than 0.015 (denoted in red). Only one specimen yielded a negative result for IgG, which is likely attributable to its collection from a patient on the first day following post-symptomatic presentation (Figure 2b). Simultaneous COVID-19 IgM/IgG testing demonstrated a sensitivity of

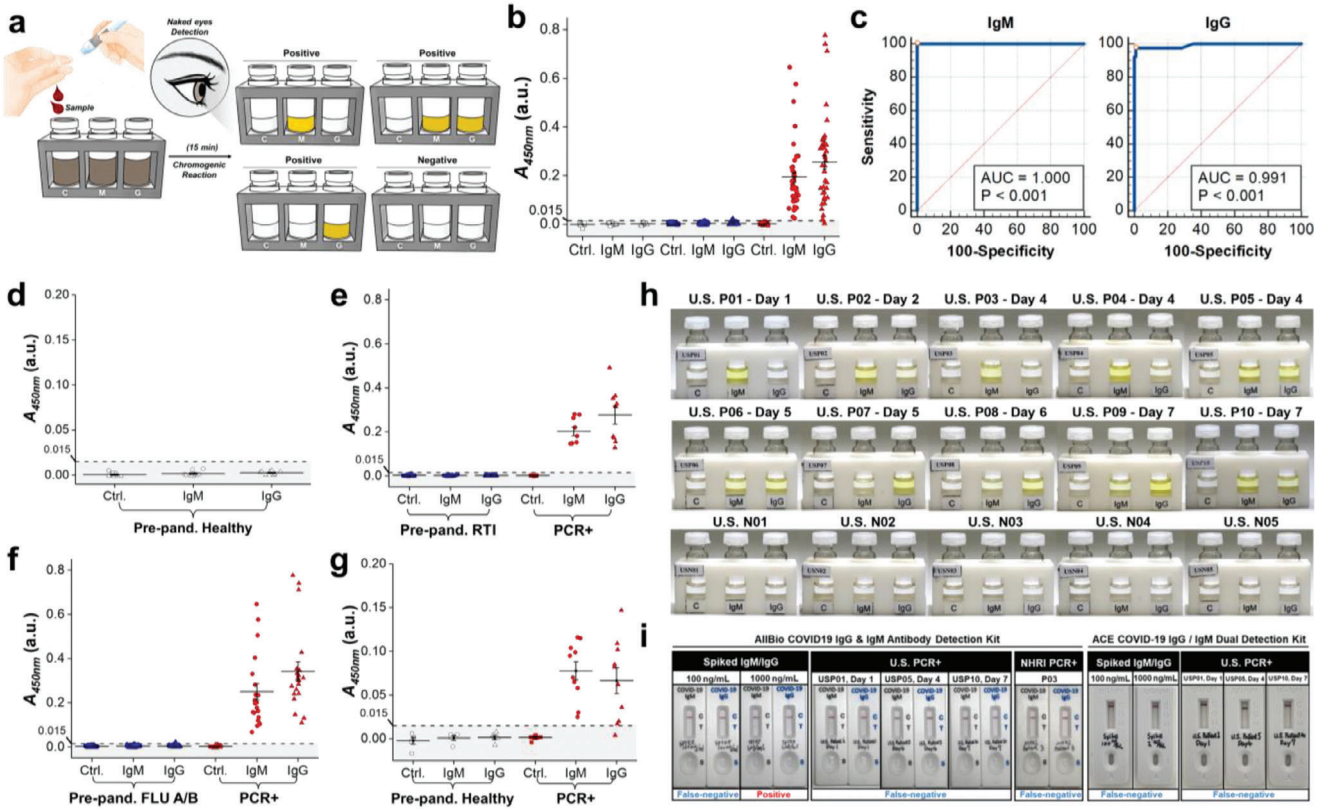

Figure 2. Comprehensive evaluation of $3LV_{COV}$ rapid diagnostic kit using 163 clinical specimens from various sources. a) All-in-one rapid testing procedures of triple vials for human anti-SARS-CoV-2 N-protein IgM/IgG antibody detection, b) Scatter interval plot of detection results for $3LV_{COV}$ based on A_{450} values, c) Receiver operating characteristic (ROC) curve analysis for human anti-SARS-CoV-2 N-protein IgM/IgG antibody detection, d) Distribution of A_{450} values for 10 pre-pandemic healthy volunteer fingertip blood samples, e) Distribution of A_{450} values for 48 samples from KMU, f) Distribution of A_{450} values for 90 positive and negative samples from NHRI, g) Distribution of A_{450} values for early infection positives and healthy negative samples from the U.S., h) The results obtained through $3LV_{COV}$ rapid diagnostic kit testing, including 5 negative samples and 10 positive samples within 7 days of symptom onset from U.S. (images taken after terminating the reaction), i) Comparing the sensitivity of the developed $3LV_{COV}$ rapid diagnostic kit with commercially available lateral flow test strips in the detection of standard samples, U.S. positive samples, and NHRI P03 positive samples. Ctrl.: negative control; PCR+: RT-qPCR-confirmed SARS-CoV-2 infections; Pre-pand. Healthy (or RTI or FLU A/B): generally healthy individuals or individuals with other respiratory tract infections (e.g., influenza A/B) prior to October 2019.

Table 1. Comprehensive sensitivity and specificity evaluation of the $3LV_{COV}$ rapid diagnostic kit using 163 clinical specimens from various sources. POS represents positive; NEG represents negative.

Summarized Sample Panels (n = 163)				
	RT-PCR POS (39)		NEG (124)	
	IgM	IgG	IgM	IgG
POS	39	38	0	0
NEG	0	1*	124	124
IgM+/IgG- Sensitivity = 100% (39/39)				
IgM-/IgG+ Sensitivity = 97.4% (38/39)				
IgM/IgG Sensitivity = 100% (39/39)				
IgM/IgG Specificity = 100% (124/124)				
* – The sample collection of 1st day after first symptom-onset (U.S. P01)				

100% (39/39) and a specificity of 100% (124/124) for positive and negative samples, respectively. The data from this study suggest that the $3LV_{COV}$ rapid diagnostic kit consistently maintains high sensitivity and specificity across a variety of assays. Following receiver operating characteristic curve (ROC) analysis of the $3LV_{COV}$ rapid diagnostic kit for IgM and IgG antibody detection,[15,16] the results indicated a mean sensitivity of 100% (95% CI = 91.0–100%) and a mean specificity of 100% (95% CI = 97.1–100%), with AUC of 1.00 (95% CI: 0.98–1.00) and an A_{450} positive cut-off value of 0.015 for IgM antibody detection; a mean sensitivity of 97.4% (95% CI = 86.5–99.9%) and a mean specificity of 99.2% (95% CI = 95.6–100%), with AUC of 0.99 (95% CI: 0.96–1.00) for IgG antibody detection (Figure 2c). The calculated Youden index J values for the detection of IgM and IgG antibodies were 1.00 and 0.97, respectively. A Youden index J value approaching 1 signifies an elevated true positive rate and true negative rate. In addition, the accuracy for IgM/IgG to be 100% and 99.38%, respectively. This outcome provides confirmation that the $3LV_{COV}$ rapid diagnostic kit exhibits exceptional performance in discriminating between positive and negative cases.

We subsequently perform a statistical analysis on specimens obtained from various sources. The 10 fingerstick blood

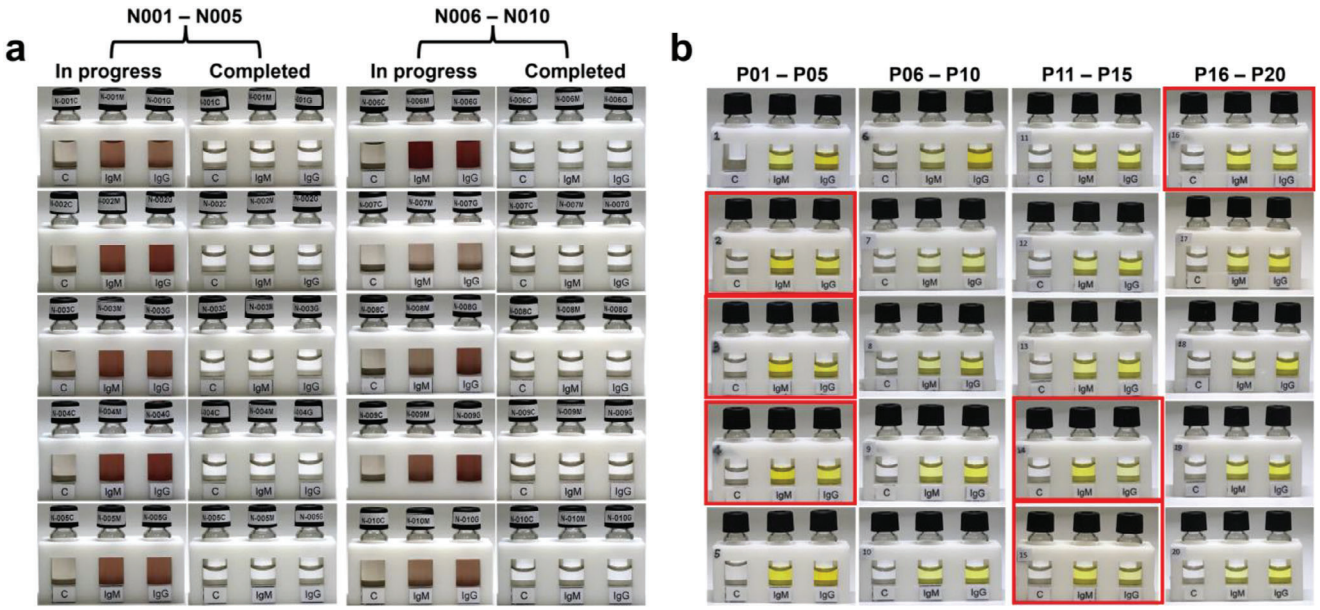

Figure 3. Visual evaluation of $3LV_{COV}$ rapid test results. a) Visual change in pre-pandemic healthy volunteer fingertip blood samples collected in 2019, showing negative reactions and transparent solutions after color development without interference from fingertip blood, b) Distinct double-strong positive reactions for human anti-SARS-CoV-2 N-protein IgM/IgG antibodies in all positive samples from NHRI, consistent with RT-qPCR determined positive test results. Samples P02, P03, P04, P14, P15, and P16, marked in red, were collected immediately after confirmation of COVID-19 positivity, corresponding to the early stages of infection.

samples from healthy volunteers were collected to assess the anti-interference capability of the $3LV_{COV}$ rapid test. These samples produced colorless and A_{450} values all below the established threshold (Figures 2d and 3a). However, when we spiked the same concentration of anti-SARS-CoV-2 N-protein IgG antibodies to both PBS and fingerstick blood for detection using the $3LV_{COV}$ rapid test, we observe that the A_{450} values obtained are not only similar but also exceed the threshold (Figure S7, Supporting Information), thus indicating that the $3LV_{COV}$ rapid diagnostic kit exhibits exceptional anti-interference properties. It can effectively detect not only serum samples but also whole blood samples, even when they contain complex components.[17,18] Then we investigated the sensitivity and specificity of $3LV_{COV}$ rapid diagnostic kit in detecting clinical serum samples from different sources. Detailed clinical data is provided in the attachment (Clinical Data List).

In the samples collected at KMU, we identified all 9 positive samples, marked in red. Specifically, K36, K38, K39, and K40 were collected from hospitalized patients who had confirmed COVID-19 diagnoses within three weeks of experiencing symptoms.[19] In contrast, samples K41, K47, K48, K49, and K50 were gathered during later stages, including periods of non-contagious recovery and asymptomatic cases. The $3LV_{COV}$ rapid diagnostic kit consistently displayed A_{450} values for both IgM and IgG significantly higher than the established threshold for all of these samples. Notably, the reagent elicited discernible color changes in 9 positive samples (Figure S8, Supporting Information). Furthermore, it maintained specificity in high-risk samples (39 negative samples, denoted in blue) for non-COVID upper respiratory infections, such as pneumonia, sepsis, and influenza, with values remaining below the established threshold (Figure 2e). The $3LV_{COV}$ rapid diagnostic kit demonstrated a sensitivity of 100% (9/9) and a specificity of 100% (39/39). However, it's important to highlight that the Abbott ARCHITECT SARS-CoV-2 IgG exhibited a lower sensitivity of only 67% (6/9), with false negative results observed for K36, K38, and K40. Similarly, the GB SARS-CoV-2 Ab ELISA IgM&IgG, which holds approvals from Taiwan Food and Drug Administration (TFDA) and CE-IVD, displayed a sensitivity of 89% (8/9), with K38 being the only sample with a false negative result (**Table 2**).

We also acquired 20 samples from the NHRI, all confirmed as COVID-19 positive via RT-qPCR. These samples were subsequently tested using the $3LV_{COV}$ rapid diagnostic kit, which consistently yielded positive results. It is essential to highlight that the reagent induced significant color changes in all 20 positive samples. Specifically, samples P02, P03, P04, P14, P15, and P16, marked in red, were collected immediately after confirmation of COVID-19 positivity, corresponding to the early stages of infection. Notably, the concentration of IgM exceeded that of IgG in these samples. The remaining 14 positive samples (P01, P05, P06, P07, P08, P09, P10, P11, P12, P13, P17, P18, P19, and P20) were predominantly collected during hospitalization and recovery phases (**Figure 3b**). In all cases, the $3LV_{COV}$ rapid diagnostic kit demonstrated consistently high A_{450} values for both IgM and IgG, significantly exceeding the established threshold. Additionally, the kit maintained its specificity against high-risk negative samples, such as those from patients with lung adenocarcinoma, sclerosing pneumocytoma, tuberculosis, and influenza, with A_{450} values remaining below the threshold (Figure 2f; Figure S9, Supporting Information). Summarily, the $3LV_{COV}$ rapid diagnostic kit demonstrated an impressive performance with a sensitivity of 100% (20/20) and a specificity of 100% (70/70). In contrast, when employing the TFDA-approved and CE-IVD marked GB SARS-CoV-2 Ab ELISA total IgM&IgG to detect the same 20 positive

Table 2. Competition of FDA/TFDA-Approved, and CE-marked products with the $3LV_{COV}$ rapid diagnostic kit for the cohort from KMU. Specificity and sensitivity analysis of Abbott ARCHITECT SARS-CoV-2 IgG, GB SARS-CoV-2 Ab ELISA Total IgM&IgG, and the present study for 48 KMU samples. POS represents positive; NEG represents negative; N/A represents not available.

Sample Panel from Kaohsiung Medical University (n = 48)				
	RT-PCR POS (9)		NEG (39)	
	IgM	IgG	IgM	IgG
POS[a]	N/A	6	N/A	0
NEG[a]	N/A	3	N/A	39
POS[b]	8		0	
NEG[b]	1		39	
POS[c]	9	9	0	0
NEG[c]	0	0	39	39

a. Abbott ARCHITECT SARS-CoV-2 IgG (FDA-approved)
IgG Sensitivity = 6/9 (67%), Specificity = 39/39 (100%)
N/A – not available

b. GB SARS-CoV-2 AbELISA Total IgM&IgG (CE-IVD, TFDA)
Sensitivity = 8/9 (89%), Specificity = 39/39 (100%)

c. this work (IgM+/IgG+)
IgM Sensitivity = 9/9 (100%), IgG Sensitivity = 9/9 (100%)
Specificity = 39/39 (100%)

samples, only 5 of them (P04, P12, P15, P18, and P20) displayed positive reactions. Surprisingly, the remaining 15 positive specimens all yielded false negative results, resulting in a detection sensitivity of only 25% (**Table 3**).

The specimens collected from KMU and NHRI exclusively consisted of serum samples from individuals diagnosed with COVID-19 during the middle and late stages of infection.[20] To ensure the robust detection sensitivity of the $3LV_{COV}$ rapid test, we imported 5 negative serum samples (denoted in blue) and 10 positive serum samples (denoted in red) within 7 days post-symptom onset (USP01–USP10) from the United States through BocaBiolistics, LLC. This was done to ensure compliance with FDA *in vitro* Diagnostic Reagent Performance Verification Guidelines. Among these 10 positive serum samples, the $3LV_{COV}$ rapid diagnostic kit consistently and accurately detected IgM-positive reactions in all 10 of them. However, it was able to detect IgG-positive reactions in only 9 (USP02~USP10) out of the 10 samples, exhibiting high A_{450} values that were notably higher than the established threshold. The $3LV_{COV}$ rapid diagnostic kit exclusively identified a positive IgM reaction but did not detect a positive IgG reaction in USP01 sample. This is attributed to the fact that USP01 represents a sample collected on the first day of symptom onset. During this early stage, either IgG antibodies have not yet been generated or their concentration is extremely low, rendering them undetectable (Figure 2g). In the corresponding images (Figure 2h), it's notable that all 10 positive samples collected within the first 7 days after symptom onset exhibited clear and distinguishable color changes. Conversely, the negative sample group remained transparent and devoid of any color. However, the FDA and CE-IVD approved chemiluminescent microparticle immunoassay (CMIA) reagent, namely the Abbott ARCHITECT SARS-CoV-2 IgG, was employed to detect the 9 positive samples (USP02~USP10). Astonishingly, only USP02 showed a positive reaction, resulting in a detection sensitivity of only 11%. Similarly, the sensitivity of EUROIMMUN SARS-CoV-2 IgG for the 4 samples (USP03, USP06, USP09, and USP10) was 0% (**Table 4**). These findings align with numerous large-scale seroepidemiological studies that have reported very low IgG seroprevalence within the first 7 days of symptom onset, often leading to false negatives.[1,2,21,22]

Table 3. Competition of FDA/TFDA-Approved, and CE-marked products with the $3LV_{COV}$ rapid diagnostic kit for the cohort from Taiwan NHRI. Specificity and sensitivity analysis of GB SARS-CoV-2 Ab ELISA Total IgM&IgG and the present study for 90 NHRI samples. POS represents positive; NEG represents negative.

Sample Panel from Taiwan NHRI (n = 90)				
	RT-PCR POS (20)		NEG (70)	
	IgM	IgG	IgM	IgG
POS[a]	20	20	0	0
NEG[a]	0	0	70	70
POS[b]	5		0	0
NEG[b]	15		70	70

a. this work (IgM+/IgG+)
IgM Sensitivity = 100% (20/20)
IgG Sensitivity = 100% (20/20)
IgM/IgG Sensitivity = 100% (20/20)
Specificity = 100% (70/70)

b. CE-IVD & TFDA-approved ELISA test kits
GB SARS-CoV-2 Ab ELISA (Total IgM&IgG)
Sensitivity = 25%
(5/20, P04, P12, P15, P18, P20)

Additionally, we also used the TFDA-approved commercial lateral flow immune rapid test strips. These included the All-Bio COVID-19 IgG & IgM antibody detection kits, and the ACE COVID-19 IgG/IgM dual detection kits, all of which are also approved by the CE-IVD. However, the testing results revealed some limitations in these conventional methods. Specifically, a 100 ng mL^{-1} standard sample resulted in false negative results for both IgM and IgG when using the conventional rapid test strip. Meanwhile, a sample with a concentration of 1000 ng mL^{-1} showed a weak positive result for IgM but a false negative for IgG on the same test strip. Additionally, the traditional test strips also demonstrated false negatives for positive samples collected on days 1 and 7 following symptom onset, as well as for the NHRI P03 positive samples. Essentially, the lateral flow test strips from the two different commercial kits tended to yield false negative results, particularly for early infections (Figure 2i). In stark contrast, the $3LV_{COV}$ rapid diagnostic kit developed in this study accurately identified all positive samples, requiring only a 5 µL sample and less than 15 min for testing which is comparable in speed to the rapid test strips. The research results thus indicate that the new $3LV_{COV}$ rapid diagnostic kit offers higher sensitivity and specificity compared to the traditional lateral flow immune rapid detection test strips.

Overall, the $3LV_{COV}$ rapid diagnostic kit demonstrated outstanding performance, achieving a sensitivity of 100% (39/39) and an equally impressive specificity of 100% (124/124) when compared to the currently approved mainstream immunoassays

Table 4. Competition of FDA/TFDA-Approved, and CE-marked products with the $3LV_{COV}$ rapid diagnostic kit for the cohort from the United States. Specificity and sensitivity analysis of Abbott ARCHITECT SARS-CoV-2 IgG, EUROIMMUN SARS-CoV-2 IgG, and the present study for 15 imported U.S. samples mostly collected within the first 7 days after symptom onset. POS represents positive; NEG represents negative; N/A represents not available.

Sample Panel Imported from U.S. (n = 15) 0 – 7 days since first symptom-onset				
	RT-PCR POS (10)		NEG (5)	
	IgM	IgG	IgM	IgG
POS[a]	10	9	0	0
NEG[a]	0	1*	5	5
POS[b]	1/9		N/A	
NEG[b]	8/9		N/A	
POS[c]	0/4		N/A	
NEG[c]	4/4		N/A	
a. this work (IgM+/IgG+) IgM Sensitivity = 100% (10/10) IgG Sensitivity = 90% (9/10) IgM/IgG Sensitivity = 100% (10/10) IgM/IgG Specificity = 100% (5/5) * – The sample collection of 1st day after first symptom-onset (U.S. P01)			FDA-approved & CE-IVD ELISA test kits b. Abbott ARCHITECT SARS-CoV-2 IgG IgG Sensitivity = 11% (1/9, U.S. P02-10) c. EUROIMMUN SARS-CoV-2 IgG IgG Sensitivity = 0% (0/4, U.S. P03, 06, 09, 10)	

available in the market. It proves to be especially suitable for diagnosing patients in the early stages of a viral infection, which is crucial for containing the spread of the pandemic.

2.3. Single Vial-Based LV Rapid Test for Anti-SARS-CoV-2 N-Protein IgM Antibody ($1LV_{COV}$) Detection

In our quest to provide the general public with a rapid, convenient, and user-friendly method for identifying ongoing infections, we have developed an improved Lab-in-a-Vial rapid diagnostic kit with single-vial tailored specifically for IgM qualitative detection. This $1LV_{COV}$ rapid diagnostic kit simplifies the process with a straightforward color-coded system (blue color for positive and transparent for negative), making it easily accessible to everyone. The entire process, from sample application to result interpretation, can be completed within a brief 12–15 min timeframe. Moreover, the generation of biohazardous waste during the testing process is addressed by safely collecting it in the absorbent pad within each individual test box (**Figure** 4a). To ensure practicality and accessibility, we've demonstrated the feasibility of mass-producing these rapid tests in medical device factories. Through three batches of trial production, totaling 2800 sets (400, 800, and 1600 sets in each batch), we've conducted relevant clinical validations. Each box is comprehensive, containing 20 tests along with essential components such as reagent dropper bottles (for detection buffer, wash buffer, chromogenic substrate, reactive control, and non-reactive control), disposable lancets, and plastic microdroppers (Figure 4b).

The primary aim of the $1LV_{COV}$ rapid diagnostic kit is to detect extremely low levels of IgM antibodies during the early stages of a SARS-CoV-2 infection. Hence, achieving the highest possible detection sensitivity is crucial. To evaluate the sensitivity, a study was conducted to determine the detection limits of these single vial-based Lab-in-a-Vial rapid tests. A series of dilutions spanning four orders of magnitude was prepared using a pure humanized anti-SARS-CoV-2 N-protein IgM antibody standard. The results indicated a significant change in intensity, amounting to ≈4 logarithmic units at 650 nm. Based on these findings, the linear detection range of the antibody was estimated to be ≈10 pg mL^{-1} to 10 ng mL^{-1}, with a LOD of 3.87 pg mL^{-1} (Figure 4c). Compared to ELISA and LFA methods, our LV rapid diagnostic platform achieves sensitivity improvements by factors of 250 and 1300, respectively.[23–25] It's essential to emphasize that these concentrations represent the levels in the original sample, rather than the levels in the sample that has been spiked into 0.8 mL of assay buffer. In practical applications, the concentration resulting from the immunosorbent process is diluted ≈160-fold, effectively placing its actual detection sensitivity in the fg mL^{-1} range. Even at this significantly lower concentration, the colorimetric reaction still displays a noticeable color change compared to the natural chromogen background. These results underscore the superior sensitivity and wide dynamic range offered by our innovative $1LV_{COV}$ rapid diagnostic kit. Additionally, further analysis was performed using the detection results of a standard sample of 100 pg mL^{-1} (anti-SARS-CoV-2 N-protein IgM antibody) from different production batches. Intra-assay variability (same sample, same batch of reagents) and inter-assay variability (same sample, different batches of reagents) were evaluated. The mean ± standard deviation (SD) and coefficient of variation (CV%) for the intra-assay variability (same sample, same batch of reagents) were calculated to be 0.0153 ± 0.0006 (A_{650nm}) and 3.76% (n = 3), respectively, while those for the inter-assay variability (same sample, different batches of reagents) were 0.0147 ± 0.001 (A_{650nm}) and 6.53% (n = 6), respectively. These findings confirm the high precision and reproducibility of this rapid test.

To evaluate the effectiveness of the mass-produced $1LV_{COV}$ rapid diagnostic kit in detecting positive COVID-19 results, we

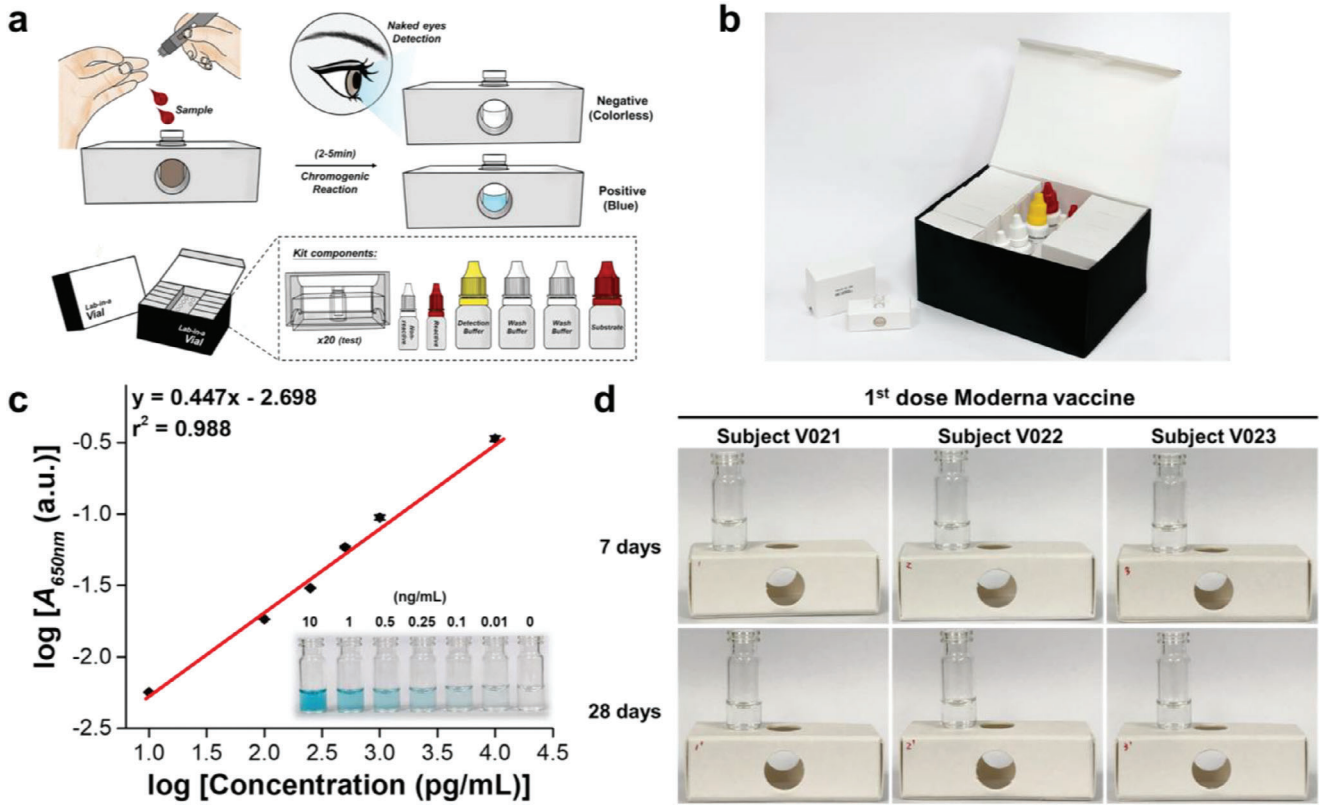

Figure 4. Single-vial 1LV$_{COV}$ IgM rapid diagnostic kits adapted for early-infection rapid screening. a) All-in-one rapid test procedures for early IgM screening, b) The product of the 1LV$_{COV}$ IgM rapid diagnostic kits under quality management system in the medical device manufacture, c) Linear calibration curve and limit of detection of the 1LV$_{COV}$ IgM rapid tests. Data are mean ± s.d.; n = 6 repeated tests, d) Visual evaluation of specificity using vaccinated specimens.

conducted a focused study on reactivity and specificity (Table S1, Supporting Information). This experiment involved 5 positive serum samples (NHRI P01-P05) and 6 positive plasma samples (U.S. P11-P16), all collected within 0–7 days after the first onset of symptoms, making a total of 11 cases. The 1LV$_{COV}$ rapid diagnostic kit successfully detected human anti-SARS-CoV-2 N-protein IgM antibody in all 5 positive serum samples (confirmed by Roche Cobas SARS-CoV-2 Test/U.S. CDC Primer) and 6 positive plasma samples (confirmed by Cepheid GeneXpert SARS-CoV-2 Test/U.S./CDC Primer), the test consistently yielded 100% sensitivity. Furthermore, we assessed the specificity of the 1LV$_{COV}$ rapid diagnostic kit using 70 high-risk negative serum samples (NHRI N01-N70) from individuals exhibiting symptoms akin to COVID-19, such as fever, cough, sore throat, and runny nose. Remarkably, in this sample panel, the test consistently yielded 100% specificity (Tables S2 and S3, Supporting Information), indicating that the potential of this 1LV$_{COV}$ rapid diagnostic kit to assist in screening for infected individuals by detecting human anti-SARS-CoV-2 N-protein IgM antibody in human serum and plasma samples.

Next, we assessed whether the 1LV$_{COV}$ rapid diagnostic kit can be effectively applied in point-of-care settings, allowing non-professionals to perform tests without prior training. To do so, we recruited 10 individuals with no prior training, who followed the instructions and conducted sample analysis (25 positive samples and 87 negative samples) in a double-blind manner (Table S4, Supporting Information). The unblinding results revealed a 100% positive concordance rate among the 25 positive samples, including 10 samples collected within 0–7 days of symptom onset. Regarding specificity, the test also demonstrated 100% specificity. The study findings suggest that this expandable, customizable, 1LV$_{COV}$ rapid diagnostic kit can be easily performed (as demonstrated in the Video S1, Supporting Information) without requiring specialized training or the use of a spectrophotometer. In summary, we analyzed a total of 36 RT-qPCR positive samples (20 serum samples from Taiwan NHRI P01-P20, 10 serum samples from U.S. P01-P10, and 6 plasma samples from U.S. P11-P16) and 157 negative serum samples using the 1LV$_{COV}$ rapid diagnostic kit. The test results demonstrated 100% specificity and sensitivity (**Table 5**). Additionally, the accuracy was 100% based on 193 real sample tests. In comparison to the inaccuracies observed with the LFP, ELISA, and CMIA reagents used in this study, this 1LV$_{COV}$ rapid diagnostic kit achieved 100% accuracy for all 193 samples, including the 16 samples collected within 0–7 days of symptom onset. This approach enables early infection detection through visual interpretation shortly after symptom onset.

Apart from the accurate detection, given the widespread COVID-19 vaccination, most individuals develop anti-SARS-CoV-2 S-protein IgG/IgM antibodies due to vaccination. Therefore, it is crucial to ensure that this 1LV$_{COV}$ rapid diagnostic kit is not interfered with by these vaccine-induced

Table 5. The evaluation of specificity and sensitivity for IgM antibody detection in 193 samples using $1LV_{COV}$ IgM rapid diagnostic kit. All kits are produced under quality management system in the medical device manufacture. POS represents positive; PT NEG represents presumptive negative.

Sample Panels from Taiwan NHRI & U.S. Import (n = 193)			
	RT-PCR POS	PT NEG	95% Confidence interval
POS	36	0	87.9% – 100%
NEG	0	157	97.0% – 100%
Sensitivity = 36/36 (100%)			
Specificity = 157/157 (100%)			
All samples are tested accurate in this rapid test system (16 cases, <7 days first-symptom onset)			

antibodies. We tested a total of 26 samples (V001-V023), including fresh fingertip or venous blood samples collected from subjects after receiving two or three doses of the vaccine (Spikevax, Moderna or Vaxzevria, AstraZeneca) at various time points ranging from one week to three months post-vaccination (Table S5, Supporting Information). All blood samples tested returned negative results, indicating 100% specificity in the vaccinated sample group. Notably, subjects V021, V022, and V023, who provided fresh venous blood samples first and fourth week after receiving the first Spikevax vaccine dose, exhibited visually distinguishable negative rapid test results using the $1LV_{COV}$ rapid diagnostic kit for on-site assessment, as shown in Figure 4d. This is primarily because current COVID-19 vaccines are designed to induce the production of anti-SARS-CoV-2 S-protein IgG/IgM antibodies, while our $1LV_{COV}$ rapid diagnostic kit or $3LV_{COV}$ rapid diagnostic kit are designed to specifically identify anti-SARS-CoV-2 N-protein IgG/IgM antibodies. Hence, there is no risk of misinterpretation or false-positive results.

2.4. Single Vial-Based Lab-in-a-Vial Rapid Diagnostic Kit for NMP22 ($1LV_{UC}$) Detection in UC

The above results confirm the effectiveness of the 1LV rapid diagnostic kit for qualitative rapid testing. To validate the versatility of this LV rapid diagnostic platform and ensure the reliability of accurate quantitative testing, we leverage the LV rapid diagnostic platform feature to rapidly convert $1LV_{COV}$ into $1LV_{UC}$ for the detection of NMP22 concentration in urine. Following the standard operating procedures of the LV rapid diagnostic platform and using the developed MiniSpec allows for the detection of NMP22 concentration in urine samples within 15 min. The MiniSpec is designed for rapid quantification (within 5 sec) of NMP22 concentrations in 1–3 urine samples simultaneously, and it can send the test reports to the attending physician and the patient via internet after the testing is completed to achieve the objectives of the Healthcare Internet of Things (H-IoT) (**Figure 5a**). To further validate the quantitative performance of the $1LV_{UC}$ rapid diagnostic kit, we conducted tests using different concentrations of NMP22 standard. While 1LV rapid diagnostic kit is capable of detecting protein biomarkers as low as 1 pg mL^{-1} with high sensitivity, in order to make it suitable for detecting physiological urinary concentration levels of NMP22 (healthy: 4.3 ± 1.5 ng mL^{-1}; UC: 28.4 ± 8.8 ng mL^{-1}),[26–30] the $1LV_{UC}$ rapid diagnostic kit study adjusted the concentration of the $PtNH_{NMP22}$ reagent. This adjustment was necessary to ensure that the detection range aligns with ng mL^{-1} concentrations, thus avoiding potential overexposure of the colorimetric response due to the inherently high-sensitivity, low-concentration detection nature of this LV detection technique.

As depicted in Figure 5b, the resulting yellow color intensified as the NMP22 concentration increased. Subsequently, we validated the sensitivity and linear detection range of the $1LV_{UC}$ rapid diagnostic kit using both a 96-well plate reader and the developed MiniSpec. The standard curves were found to be linear and fell within the range of 0.1–100 ng mL^{-1} (with $r^2 = 0.998$ for the 96-well plate reader and $r^2 = 0.997$ for MiniSpec; see Figure S10, Supporting Information). The results indicate that the signals recorded using the MiniSpec exhibit the same accuracy and sensitivity as those recorded using a 96-well plate reader. The detection ranges recorded by both the 96-well plate reader and the MiniSpec are sufficient for assessing the risk and prognosis of UC based on the NMP22 concentration in urine. Additionally, they allow for at least a 100-fold dilution of the original urine sample for analysis.

In order to prove the reliability of $1LV_{UC}$ rapid diagnostic kit combined with the MiniSpec, a total of 42 urine samples (15 samples collected from UC patients and 27 samples collected from healthy donors) were obtained from Linkou Chang Gung Memorial Hospital, and then their NMP22 concentrations were determined by $1LV_{UC}$ rapid diagnostic kit through MiniSpec autocalculation. The detection results from the urine samples of UC patients are displayed in Figure 5c. In comparison to the clear solution of the negative control group, the solutions in the vials of the UC patient group all exhibit a significant yellow color after the reaction, signifying the presence of a high concentration of NMP22 in the urine samples from UC patients. Furthermore, urine samples from healthy donors themselves contain NMP22 concentrations well below the threshold concentration. Consequently, the solutions in all vials appear very light yellow or even as clear as the negative control group, as depicted in Figure 5d. The above results demonstrate the excellent sensitivity and specificity of the $1LV_{UC}$ rapid diagnostic kit in detecting NMP22 in the urine of UC patients. From the data in the linear detection range, it is evident that higher A_{450} values are associated with greater concentrations of NMP22 in urine samples, indicating a robust positive correlation. Consequently, we can employ the MiniSpec instrument equipped with the $1LV_{UC}$ rapid diagnostic kit to analyze A_{450} values from a substantial number of urine samples from healthy donors. This will enable us to establish an A_{450} threshold for evaluating whether the NMP22 content in the subject's urine sample falls within the normal range or is abnormal. The A_{450} values were first measured by a 96-well plate reader, the obtained scatter interval plot revealed that all A_{450} values for $1LV_{UC}$ rapid diagnostic kits corresponding to negative control group (denoted in square) and healthy subjects (denoted in circle) were below the threshold of 0.019. In contrast, all A_{450} values for $1LV_{UC}$ rapid diagnostic kits corresponding to UC patients were significantly greater than 0.019 (denoted in triangle), indicating that patients with UC indeed overexpress NMP22 (Figure 5e). Following that, we proceed to analyze the A_{450} values using

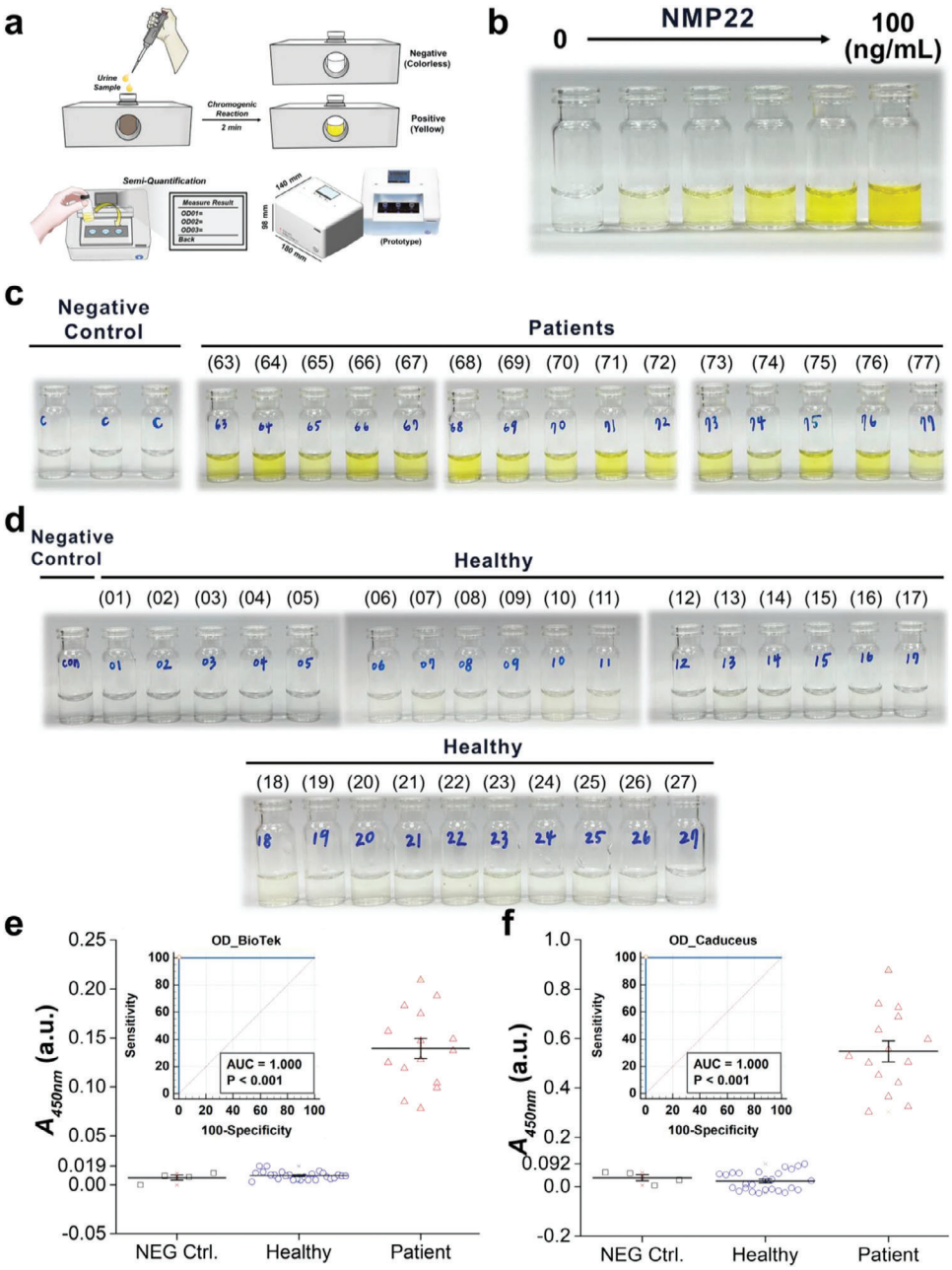

Figure 5. Analytical performance and evaluation of $1LV_{UC}$ rapid diagnostic kit for NMP22 protein detection in UC. a) All-in-one rapid testing procedures for NMP22 detection and quantification in urine samples using MiniSpec, b) The visual detection results of NMP22 standards: A correlation is shown between the concentration of NMP22 standards (0, 5, 10, 25, 50, 100 ng mL^{-1}) and the color intensity of the solution, with higher concentrations resulting in a deeper color, c) Colorimetric change in actual urine samples from UC patients: These 15 samples, which contain the NMP22 biomarker, show significant color change compared to the clear solution of the negative control group, d) Colorimetric change in normal individuals urine samples: It depicts the comparatively less pronounced color change in urine samples from normal individuals, which contain NMP22 at lower concentrations. There's no significant color difference when compared to the transparent negative control group, e) Statistical analysis and ROC curve analysis of 46 urine sample results by the 96-well plate reader, f) Statistical analysis and ROC curve analysis of 46 urine sample results by the MiniSpec.

MiniSpec, the obtained scatter interval plot revealed that all A_{450} values for $1LV_{UC}$ rapid diagnostic kits corresponding to negative control group (denoted in square) and healthy subjects (denoted in circle) were below the threshold of 0.092, and all A_{450} values for $1LV_{UC}$ rapid diagnostic kits corresponding to UC patients were significantly greater than 0.092 (denoted in triangle), which has the same trend as the analysis using a 96-well plate reader (Figure 5f). The ROC analysis by the respective thresholds for them indicated a mean sensitivity of 100% (95% CI = 78.2–100%) and a mean specificity of 100% (95% CI = 88.4–100%), with AUC of 1.00 (95% CI: 0.92–1.00) (Figure 5e,f, insets). Additionally, for the $1LV_{UC}$ rapid diagnostic kit, the accuracy was also 100% for

42 samples at the set threshold. The results demonstrate that the precision and stability of A_{450} measurements using MiniSpec are comparable to that of a 96-well plate reader, and the $1LV_{UC}$ rapid diagnostic kit exhibits exceptional sensitivity in identifying UC.

3. Discussion

Immunological assays, particularly ELISA and LFA, are the main methods for detecting cancer marker proteins, viral antigens, and immune antibodies in routine diagnostics. LFA is favored for rapid testing due to its simplicity and speed, and has been extensively used for quick SARS-CoV-2 detection. However, its sensitivity and specificity for early infection detection are suboptimal.[3,4,17,31–33] The U.S. FDA's Emergency Use Authorization documents indicate that commercially available antibody rapid tests, with sensitivity typically below 30% in the first 7 days of infection or symptom onset, are supplementary tools for pandemic surveillance rather than primary diagnostic tools, primarily due to the high risk of false negatives.[34] This low sensitivity also limits LFA's suitability for cancer risk assessment. In contrast, traditional ELISA, offering superior sensitivity for all types of protein markers, is more complex and time-consuming, requiring professional execution in medical centers. The absence of a technology combining ELISA and LFA's advantages has restricted the implementation of POCT. Our group introduces the LV rapid diagnostic platform as an innovative approach for rapid, real-time fluidic protein biomarker testing, marking a significant breakthrough. This platform integrates the concept of an analytical laboratory in a vial (LV), nanozymes with high stability and catalytic activity (PtNH), and portable spectrometer (MiniSpec) together, facilitating the rapid development of diverse test kits. Each kit is specifically tailored for distinct protein molecules, addressing the limitations of ELISA and LFA by balancing speed, sensitivity, and practicality.

The LV rapid diagnostic platform's enhanced detection sensitivity could revolutionize rapid diagnostics, especially in resource-limited settings, offering invaluable on-site, real-time testing capabilities for disease outbreak management and routine health testing. This rapid testing capability is crucial for timely clinical decision-making and patient care. Our clinical specimen verification data confirms the successful design and feasibility of the LV rapid diagnostic platform for clinical use. Its modular design allows for versatile applications; antigens can be easily immobilized within the vials to detect antibody concentrations in specimens, or antibodies can be immobilized to measure antigen concentrations in specimens. This LV rapid diagnostic platform is capable of analyzing various specimen forms, including serum, blood, saliva, and urine. Currently, the LV rapid diagnostic platform has been effectively used to measure IgG/IgM antibody levels in serum samples post-SARS-CoV-2 infection (Figure 2), NMP22 concentrations in urine samples from UC patients (Figure 5), and HE4 levels (specific data not included here) in serum samples of breast cancer patients, with the results being notably impressive. The immense potential of the LV rapid diagnostic platform for expanding biomarker detection opens new avenues for personalized medicine. For instance, it could reduce delayed medical consultations for cancer patient post-treatment, lowering the risk of tumor recurrence or metastasis. Furthermore, the significance of the LV rapid diagnostic platform in Health IoT (H-IoT) cannot be understated, especially in underserved or rural areas. The cost-effectiveness of this method, relative to traditional high-sensitivity ELISA, is highlighted by the approximate cost of one test at $0.7–1.0 USD and a portable spectrometer at ≈$200 USD. This affordability has the potential to democratize healthcare services, facilitating diagnostics and monitoring outside conventional clinical settings. This not only eases the strain on healthcare facilities but also offers a significant advantage to patients with mobility issues or those living in remote locations. The LV rapid diagnostic platform now is poised to develop rapid testing for exosomes and extend to precise screenings for hard-to-diagnose cancers, like pancreatic and ovarian, and those with high recurrence risks, such as breast, lung, and colorectal cancers. In summary, the LV rapid diagnostic platform represents a substantial advancement in protein biomarker testing, potentially transforming diagnostics in point-of-care settings and establishing a new standard for protein biomarker testing.

4. Conclusion

The LV rapid diagnostic platform constitutes a significant breakthrough in the detection of protein biomarkers, including antibodies and antigens, in bodily fluids. It ingeniously integrates a colorimetric biosensor for enhanced sensitivity, a user-friendly operation cassette, and a portable spectrometer for precise quantification, thereby addressing the critical demand for efficient biomarker detection. At its core, the platform incorporates the innovative LV colorimetric biosensor, which improves sensing performance by enabling uniform biomolecule capture on the inner walls of vials, thus increasing the surface area available for molecule capture. The biosensor is optimized with PtNH to achieve a broad detection range from 10 pg mL^{-1} to 10 ng mL^{-1}, exhibiting high linearity (r^2 = 0.988) and an ultra-low LOD of 3.87 pg mL^{-1}. The detection process is expedited, completing within 15 min, and the LV rapid diagnostic kits demonstrate high specificity and stability, remaining effective for up to 1 year in storage. This biosensor not only facilitates early diagnosis of diseases such as SARS-CoV-2 infection and urothelial carcinoma but also complements existing methodologies including RT-qPCR, ELISA, and LFA. Its modularity and scalability render it suitable for diverse protein biomarker detections. An essential enhancement to this platform is the MiniSpec quantitative platform, a portable and wireless device that extends the benefits of the LV rapid diagnostic platform—speed, cost-efficiency, and simplicity—to POCT applications. This integration enables rapid, accurate, and user-friendly detection of anti-SARS-CoV-2 N-protein IgM/IgG antibodies in serum and NMP22 in urine. In conclusion, the amalgamation of the LV rapid diagnostic platform with the MiniSpec quantitative platform heralds a paradigm shift in rapid protein biomarker detection. It is poised for further development and broader application in detecting an extensive range of protein biomarkers and clinical samples in the foreseeable future. This biodetection technology has the potential to significantly impact the medical field.

5. Experimental Section

Vial Production Under Quality Management System: All batches, comprising hundreds of in vitro diagnostic vial kits for clinical tests, were authorized for production by medical device manufacturers in Taiwan. The manufacturing processes adhere to the quality management system (QMS) standards, which encompass good manufacturing practice/good distribution practice (GMP/GDP), quality assurance from the College of American Pathologists (CAP), and certifications from the International Organization for Standardization – ISO 13485:2016, ISO 9001:2015, as well as CNS 12681:2016.

Manufacture of Diagnostic Vials: Initially, a solution of Tris-buffered saline containing 0.1% Tween 20 detergent (TBST) was introduced into a 1.5 mL glass vial to remove any dirt and grease from the glass surface. This was achieved using an ultrasonic cleaner with high-amplitude oscillation for a duration of 15 min. Afterward, the vial was rinsed multiple times with deionized water (DI-H_2O). Acetone was then added, and the vial was subjected to ultrasonic cleaning for another 15 min to remove the remaining impurities. The vial was subsequently rinsed three times with DI-H_2O to eliminate any remaining organic solvents and then dried. The glass vial was immersed in 95% ethanol and agitated on a rotary shaker at room temperature for 1 h. Following this treatment, the vial exhibiting a negative surface potential was considered adequately cleaned.

A 10 wt.% aqueous solution of bPEI was initially prepared and subsequently homogenized via high-amplitude oscillation in an ultrasonic cleaner. This was followed by dilution to the requisite concentrations of 0.5, 0.75, and 1 wt.%. Subsequently, 0.1 mL of different concentrations of bPEI was added to each glass vial and allowed to react at room temperature for 2 h. Electrostatic adsorption facilitated the uniform coating of bPEI on the glass surface.[35,36] Vials were rinsed several times with DI-H_2O to remove any unabsorbed bPEI polymer. For enhanced adhesion and to ensure the binding of the amine groups (-NH_2) to the glass surface, the bPEI-coated vials were heated on a plate at 80 °C for a minimum of 15 min, then cooled to room temperature. The presence of amine groups on the surface was confirmed using the TNBS assay.[37]

For the COVID-19 rapid test, the SARS-CoV-2 nucleocapsid protein (N-protein) was employed as the capture biomolecule. Owing to its profuse negative surface charges, it was electrostatically and stably adsorbed onto the bPEI-coated vial's surface. Subsequent to this adsorption, any unbound surfaces were blocked using a PBS solution containing more than 0.5 wt.% BSA. After these steps, the vials were prepared for the rapid detection of anti-SARS-CoV-2 N-protein IgM and IgG antibodies in serum samples.

For the UC rapid test, the vial preparation procedure remained consistent with the above. However, the capture molecule was substituted with the anti-NMP22 antibody. Once prepared, the vials were ready for the rapid detection of NMP22 in urine samples.

Preparation of a Nanozyme-Based Signal with High Catalytic Activity (Detection Buffer): In this study, PtNH was prepared as nanozymes, aiming to substitute the conventional HRP. The PtNH were synthesized employing a hydrothermal method. Initially, an aqueous solution of BSA at a concentration of 20 mg mL^{-1} was prepared, followed by the addition of ethanol (95% V/V). This mixture, upon turning turbid, was heated to 70 °C and continuously stirred for 30 min, resulting in a stabilized BSA nanoparticles (BSA NPs) solution.[38] Free BSA and ethanol were subsequently removed from the BSA NPs through centrifugation (10 000 g, 15 min) using DI-H_2O. Next, 100 mg of polyvinylpyrrolidone (PVP) was dissolved in 10 mL DI-H_2O, to which the BSA nanoparticles were added. After stirring evenly, the mixture was incubated at 75 °C for 5 min. This was followed by the addition of 25 mg H_2PtCl_6, stirring and mixing continuously for 30 min. Upon obtaining a turbid yellow mixture, it was promptly heated to 185 °C for 15 min. The resultant product, a platinum shell-BSA core complex, appeared as a dark-brown PtNH nanozyme. This was washed thrice using deionized water and centrifuged (10 000 g, 15 min). The absorbance of the prepared nanozyme was adjusted to OD_{290nm} = 0.5 in a 0.5 wt.% PVA aqueous solution.

The kinetic parameters of the reactions were determined using a steady-state assay. The initial reaction rates of PtNH and HRP for the reactions with different concentrations of H_2O_2 (6, 15, 30, 60, 150, and 300 µM) were measured. The kinetic parameters (K_m and V_{max}) were calculated using the Lineweaver–Burk plot of the Michaelis–Menten equation:

$$\frac{1}{V_0} = \frac{K_m}{V_{max}} \times \frac{1}{[S]} + \frac{1}{V_{max}} \quad (1)$$

where V_0 represents the apparent initial reaction rate, K_m denotes the apparent Michaelis–Menten constant, V_{max} is the maximum reaction rate, and *[S]* refers to the substrate concentration.

Preparation of Antibody Conjugated PtNH Nanozyme: For the COVID-19 rapid test, the PtNH nanozyme was modified through covalent bonding with either thiolated anti-human IgM ($Fc_{5\mu}$-specific) antibodies or anti-human IgG (Fc-specific) antibodies. Initially, anti-human IgM antibodies or anti-human IgG antibodies were thiolated using 10 mM of Traut's reagent (2-iminothiolane) to introduce sulfhydryl groups. Subsequently, the PtNH nanozyme was activated with of sulfo-succinimidyl 4-(*N*-maleimidomethyl)cyclohexane-1-carboxylate (sulfo-SMCC) solution (50 µg mL^{-1}) for 2 h in darkness, followed by incubation with different concentrations of the thiolated antibodies (either anti-human IgM or anti-human IgG) for an additional 2 h. After this modification, any unbound surfaces were blocked by resuspending the nanozyme in a PBS solution containing 1 wt.% BSA, thereby forming the detection buffer (either $PtNH_{IgM}$ or $PtNH_{IgG}$).

For the UC rapid test, the PtNH nanozyme was similarly modified, this time with the thiolated anti-NMP22 antibody through covalent bonding. After this, any unattached surfaces were blocked by resuspending the nanozyme in a PBS solution containing 1 wt.% BSA, resulting in the detection buffer ($PtNH_{NMP22}$).

The Design of MiniSpec for LV Rapid Diagnostic Platform in NMP22 Detection: The concentration of NMP22 in urine samples was determined by measuring the absorbance intensity at 450 nm using the MiniSpec, which has dimensions of 180 × 140 × 98 mm. A 75 mW laser diode emitting at a wavelength of 450 nm served as the light source. This light was evenly divided by three neutral density (ND) filters into four beams—A, B, C, and R—all with the same laser power (see Figure S11, Supporting Information). Beams A, B, and C were reflected by three ND filters at incidence angles of 45°, traversed the sample solutions, and were then detected by photodiodes (PDs). The transmittance of the laser beam passing through the ND filters was monitored by a fourth PD as the reference beam (R). Three vials containing the sample solutions were inserted vertically into the sample holder at the beam paths of A, B, and C, respectively.

All-in-one Procedure of LV Rapid Diagnostic Kit: The LV rapid test employs a vial-based immunoassay, akin to ELISA, tailored for the qualitative identification of antibodies and antigens, including IgM and IgG antibodies specific to SARS-CoV-2 N-protein and cancer biomarkers like NMP22 (for UC diagnosis). To enhance user experience and streamline waste collection during the detection process, an operation cassette was developed that houses the vials (Figure 1). In this study, three distinct LV rapid test were designed tailored to specific detection objectives:

1) To ascertain the SARS-CoV-2 infection status, a rapid test was developed encompassing three vials within an operation cassette for concurrent detection of IgM and IgG antibodies against the SARS-CoV-2 N-protein. A positive result from the IgM vial typically indicates an acute or early-stage infection, whereas a positive result from the IgG vial suggests a mid-to-late stage of infection.
2) To swiftly diagnose SARS-CoV-2 infection during its early stages, a rapid test was devised with a singular vial within a detection box dedicated to detecting the IgM antibody against the SARS-CoV-2 N-protein. A positive result from this IgM vial generally signals an acute or early-stage infection occurring within 5 days.
3) To expediently evaluate the risk of recurrence following UC surgery, a rapid test was crafted incorporating a single vial within an operation cassette for the identification of the UC biomarker NMP22. This vial was subsequently placed in the specially designed MiniSpec, enabling rapid measurement of NMP22 concentrations in urine.

Here, the determination of SARS-CoV-2 infection status was used as an illustrative example. Prior to beginning the procedure, three pre-coated vials with SARS-CoV-2 N-protein were securely placed in their respective slots within the operation cassette, namely Control, IgM, and IgG. These vials were then filled with 0.8 mL (equivalent to 16 drops) of the detection buffer, either $PtNH_{IgM}$ or $PtNH_{IgG}$, dispensed from dropper bottles. Following this, 5 microliters of the sample were added to both the IgM and IgG vials using a plastic microdropper. The operation cassette lid, equipped with an absorbent pad, was then firmly closed. To ensure uniform mixing, the box was gently agitated and then left to sit undisturbed for 10 min. The cassette was subsequently inverted and tapped on a stable surface, enabling the liquid from each vial to be absorbed by the pad. Each vial was then treated with 1 mL of wash buffer (equivalent to 20 drops), dispensed from a dropper bottle. The cassette was closed, gently shaken, and once again inverted to direct the liquid onto the absorbent pad. The final step involves adding 0.5 mL of the chromogen reagent (TMB/H_2O_2) to each vial, allowing a 2-min interval for result visualization. This LV rapid test eliminates the need for professional pipetting, additional waste liquid recovery containers, and intricate ELISA washing stages. Furthermore, the chromogenic reaction can be halted using 1 M HCl. The resultant detection can be visually inspected or evaluated using spectrometers, offering qualitative and semi-quantitative analyses, respectively.

Biological Samples: To evaluate the accuracy of the LV rapid test for clinical applications in detecting SARS-CoV-2 infections, 45 serum samples were obtained from patients with RT-qPCR-confirmed SARS-CoV-2 infections. 206 negative serum samples were also collected from generally healthy individuals and individuals with other respiratory tract infections (e.g., influenza A/B) prior to October 2019. These samples were sourced from the Human Biobank Platform of the Taiwan National Health Research Institute (NHRI) and Kaohsiung Medical University (KMU), as well as imported U.S. specimens approved by the Taiwan Ministry of Health and Welfare from BocaBiolistics, LLC & Access Biologicals, LLC. Additionally, 26 fresh fingerstick blood samples from vaccinated subjects with no prior history of COVID-19 were obtained from Chang Gung Memorial Hospital, Linkou.

To evaluate the accuracy of the LV rapid test and its applicability for clinical use in assessing the risk of recurrence following UC surgery by detecting NMP22, 15 urine samples were collected from confirmed UC patients and 27 urine samples from healthy individuals from Chang Gung Memorial Hospital, Linkou.

All samples used in this study were collected with the consent of the Chang Gung Medical Foundation Human Experiment Ethics Committee for clinical trials and research; the IRB case numbers were 202000986B0 for SARS-CoV-2 and 202102331B0C101 for UC. Additionally, the storage and transport of serum specimens adhered to guidelines from the Centers for Disease Control and Prevention in Taiwan (Taiwan CDC). All serum specimens were heat-sterilized at 56 °C for 30 min before use.

Double-Blind Study for IgM Antibody Detection Using LV Rapid Test: According to the Taiwan NHRI and Taiwan CDC, serological samples were collected from SARS-CoV-2 RT-qPCR positive patients (NHRI P06-P20 & U.S. P01-P10, 0–7 days post symptom onset) and healthy individuals from the pre-COVID-19 pandemic period (U.S. N01-N87). In total, 25 positive and 87 negative clinical serum specimens were evaluated in a double-blind study using LV rapid test for IgM antibody detection. A trusted third party randomly arranged the samples (NO.1 – NO.112), which were then distributed to ten operators responsible for conducting the tests and interpreting the results. Each rapid test required 5 µL of serum sample, following the aforementioned operation procedure. An independent researcher, who wasn't involved in sample assignment or result interpretation, conducted the unblinding process. This was to ensure that there was no subjective influence on the results by any operators or researchers familiar with the sample details.

Specificity Studies of LV Rapid Test: Using U.S. positive and negative samples endorsed by the Taiwan CDC and sourced from BocaBiolistics, LLC & Access Biologicals, LLC, serological samples were taken from SARS-CoV-2 RT-qPCR positive patients (U.S. P01-P10) within 1–7 days following the first symptom onset. Samples were also taken from individuals presumed negative prior to the COVID-19 pandemic. a total of 10 positive and 10 negative clinical serum specimens were tested, which were spiked with fresh fingerstick blood from healthy individuals (5 µL serum + 5 µL fingerstick blood/test), using the LV rapid diagnostic kit and following the operation procedure described earlier (Table S1, Supporting Information).

Additionally, based on the vaccinated panel supplied by Linkou Chang Gung Memorial Hospital, all serological samples came from healthy individuals who had never contracted SARS-CoV-2 (V001-V023). A total of 26 clinical fingerstick/venous blood specimens (5 µL blood/test) were analyzed using the LV rapid test, adhering to the previously mentioned operation procedure.

Data Analysis: After conducting rapid testing procedures, a 96-well plate reader (SpectraMax M2) was used to scan the reacted chromogenic substrate solution in each test, generating absorbance data. The absorbance values were then used from the detection results of a series of standard antibodies to plot detection curves through linear regression. The limit of detection (LOD) was calculated using the formula $LOD = 3\sigma/m$, where σ is the standard deviation of blank samples and m is the slope of the calibration curve.[39] The data from clinical sample studies were analyzed to determine cutoffs using ROC curve analysis with MedCalc Statistical Software version 20.019 (MedCalc Software). The Youden index J is a statistical measure, ranging from 0 to 1, employed to evaluate the performance of diagnostic tests. A higher Youden index J indicates greater test accuracy. The formula for the Youden index is J = Sensitivity + Specificity − 1, where Sensitivity denotes the true positive rate, and Specificity represents the true negative rate. The optimal threshold was identified using the Youden Index, which corresponds to the point on the ROC curve that was closest to the top-left corner [i.e., the point (0,1)]. This point represents the threshold that maximizes the difference between true positive rate and false positive rate, thus providing the best cut-off value. This analysis facilitated the optimization of the sensitivity and specificity of the LV rapid test. This analysis helped optimize the sensitivity and specificity of the LV rapid test. Additionally, to calculate accuracy, first identify the values of True Positives (TP), False Positives (FP), True Negatives (TN), and False Negatives (FN) from the confusion matrix. Sum the values of TP and TN to obtain the total number of correct predictions. Next, sum all the values (TP, FP, TN, and FN) to determine the total number of instances. Finally, divide the number of correct predictions by the total number of instances to determine the accuracy.

Statistical Analysis: The data were expressed as the mean ± SD on the basis of at least three independent experiments. Statistical analysis was performed using Student's t-test. Differences were considered statistically significant if $p < 0.05$.

Supporting Information

Supporting Information is available from the Wiley Online Library or from the author.

Acknowledgements

N.-S.L. and Y.-P.H. contributed equally to this work. This work was financially supported by the National Science and Technology Council and National Health Research Institutes, Taiwan (R.O.C.), for the financial assistance provided (NSTC110-2823-8-110-001, NSTC111-2218-E-182A-002, NSTC112-2628-B-006-015, and NHRI-EX113-11226EI). The authors express the gratitude to Ms. Mi-Chi Tsai for her assistance with administrative works and laboratory management and Chang Gung Memorial Hospital Microscopy Core Laboratory for the excellent assistance of TEM. The authors also appreciate the assistance of Ms. Jesse Chih-Wei Lin during the product commercialization process.

Conflict of Interest

The authors declare no conflict of interest.

Data Availability Statement

The data that support the findings of this study are available from the corresponding author upon reasonable request.

Keywords

Lab-in-a-Vial (LV), nanozymes, point-of-care testing (POCT), SARS-CoV-2, urothelial carcinoma (UC)

Received: February 2, 2024
Revised: June 25, 2024
Published online: August 6, 2024

[1] A. Bryan, G. Pepper, M. H. Wener, S. L. Fink, C. Morishima, A. Chaudhary, K. R. Jerome, P. C. Mathias, A. L. Greninger, *J. Clin. Microbiol.* **2020**, *58*, e00941.
[2] S. Meschi, F. Colavita, L. Bordi, G. Matusali, D. Lapa, A. Amendola, F. Vairo, G. Ippolito, M. R. Capobianchi, C. Castilletti, I. N. team, *J. Clin. Virol.* **2020**, *129*, 104539.
[3] C. Parolo, A. de la Escosura-Muñiz, A. Merkoçi, *Biosens. Bioelectron.* **2013**, *40*, 412.
[4] C. Huang, T. Wen, F. J. Shi, X. Y. Zeng, Y.-J. Jiao, *ACS Omega* **2020**, *5*, 12550.
[5] K. Ng, K. Vinnakota, A. Sharma, J. Kelly, P. Dasgupta, N. Vasdev, *Nat. Rev. Urol.* **2021**, *18*, 185.
[6] S. F. Shariat, C. Savage, T. F. Chromecki, M. Sun, D. S. Scherr, R. K. Lee, G. Lughezzani, M. Remzi, M. J. Marberger, P. I. Karakiewicz, A. J. Vickers, *Cancer* **2011**, *117*, 2892.
[7] J. Yang, J. Suo, H. Gao, *Cancer Research and Clinic* **2020**, *6*, 772.
[8] N. Sethuraman, S. S. Jeremiah, A. Ryo, *JAMA, J. Am. Med. Assoc.* **2020**, *323*, 2249.
[9] N. Ravi, D. L. Cortade, E. Ng, S. X. Wang, *Biosens. Bioelectron.* **2020**, *165*, 112454.
[10] Y. Chong, H. Ikematsu, N. Tani, Y. Arimizu, H. Watanabe, Y. Fukamachi, A. Yonekawa, S. Iwasaka, R. Nishida, Y. Eriguchi, N. Miyake, S. Shimoda, Y. Nagasaki, N. Shimono, K. Akashi, *Viruses* **2021**, *15*, 13.
[11] X. Wu, H. Yue, Y. Zhang, X. Gao, X. Li, L. Wang, Y. Cao, M. Hou, H. An, L. Zhang, S. Li, J. Ma, H. Lin, Y. Fu, H. Gu, W. Lou, W. Wei, R. N. Zare, J. Ge, *Nat. Commun.* **2019**, *10*, 5165.
[12] J. Liang, M. Y. Bin Zulkifli, J. Yong, Z. Du, Z. Ao, A. Rawal, J. A. Scott, J. R. Harmer, J. Wang, K. Liang, *J. Am. Chem. Soc.* **2022**, *144*, 17865.
[13] D. Liang, Y. Wang, K. Qian, *Interdiscip. Med.* **2023**, *1*, 20230020.
[14] Y. Wang, B. Li, T. Tian, Y. Liu, J. Zhang, K. Qian, *Trends. Analyt. Chem.* **2022**, *149*, 116565.
[15] K. H. Zou, A. J. O'Malley, L. Mauri, *Circulation* **2007**, *115*, 654.
[16] R. Mardani, A. A. Vasmehjani, F. Zali, A. Gholami, S. D. M. Nasab, H. Kaghazian, M. Kaviani, N. Ahmadi, *Arch. Acad. Emerg. Med.* **2020**, *8*, e43.
[17] Z. Li, Y. Yi, X. Luo, N. Xiong, Y. Liu, S. Li, R. Sun, Y. Wang, B. Hu, W. Chen, Y. Zhang, J. Wang, B. Huang, Y. Lin, J. Yang, W. Cai, X. Wang, J. Cheng, Z. Chen, K. Sun, W. Pan, Z. Zhan, L. Chen, F. Ye, *J. Med. Virol.* **2020**, *92*, 1518.
[18] L. Brown, R. L. Byrne, A. Fraser, S. I. Owen, A. I. Cubas-Atienzar, C. T. Williams, G. A. Kay, L. E. Cuevas, J. R. Fitchett, T. Fletcher, *Sci. Rep.* **2021**, *11*, 7754.
[19] M. R. Benzigar, R. Bhattacharjee, M. Baharfar, G. Liu, *Anal. Bioanal. Chem.* **2021**, *413*, 2311.
[20] H. Hou, T. Wang, B. Zhang, Y. Luo, L. Mao, F. Wang, S. Wu, Z. Sun, *Clin. Transl. Immunology* **2020**, *9*, e1136.
[21] D. L. Ng, G. M. Goldgof, B. R. Shy, A. G. Levine, J. Balcerek, S. P. Bapat, J. Prostko, M. Rodgers, K. Coller, S. Pearce, S. Franz, L. Du, M. Stone, S. K. Pillai, A. Sotomayor-Gonzalez, V. Servellita, C. S. S. Martin, A. Granados, D. R. Glasner, L. M. Han, K. Truong, N. Akagi, D. N. Nguyen, N. M. Neumann, D. Qazi, E. Hsu, W. Gu, Y. A. Santos, B. Custer, V. Green, et al., *Nat. Commun.* **2020**, *11*, 4698.
[22] M. Pollán, B. Pérez-Gómez, R. Pastor-Barriuso, J. Oteo, M. A. Hernán, M. Pérez-Olmeda, J. L. Sanmartín, A. Fernández-García, I. Cruz, N. F. de Larrea, *Lancet* **2020**, *396*, 535.
[23] W. W. W. Hsiao, T. N. Le, D. M. Pham, H. H. Ko, H. C. Chang, C. C. Lee, N. Sharma, C. K. Lee, W. H. Chiang, *Biosensors* **2021**, *11*, 295.
[24] B. A. Trombetta, S. E. Kandigian, R. R. Kitchen, K. Grauwet, P. K. Webb, G. A. Miller, C. G. Jennings, S. Jain, S. Miller, Y. Kuo, T. Sweeney, T. Gilboa, M. Norman, D. P. Simmons, C. E. Ramirez, M. Bedard, C. Fink, J. Ko, E. J. De León Peralta, G. Watts, E. Gomez-Rivas, V. Davis, R. M. Barilla, J. Wang, P. Cunin, S. Bates, C. Morrison-Smith, B. Nicholson, E. Wong, L. El-Mufti, et al., *BMC Infect. Dis.* **2021**, *21*, 580.
[25] G. K. Oluka, P. Namubiru, L. Kato, V. Ankunda, B. Gombe, M. Cotten, M. Musenero, P. Kaleebu, J. Fox, J. Serwanga, C. J. S., *Front. Immunol.* **2023**, *14*, 1113194.
[26] N. Miyanaga, H. Akaza, S. Ishikawa, M. Ohlani, R. Noguchi, K. Kawai, K. Koiso, M. Kobayashi, A. Koyama, T. Takahashi, *Eur. Urol.* **1997**, *31*, 163.
[27] S. F. Shariat, M. J. Marberger, Y. Lotan, M. Sanchez-Carbayo, C. Zippe, G. Lüdecke, H. Boman, I. Sawczuk, M. G. Friedrich, R. Casella, *J. Urol.* **2006**, *176*, 919.
[28] D. Wu, Y. Wang, Y. Zhang, H. Ma, T. Yan, B. Du, Q. Wei, *Sci. Rep.* **2016**, *6*, 24551.
[29] R. Pichler, G. Tulchiner, J. Fritz, G. Schaefer, W. Horninger, I. Heidegger, *Int. J. Med. Sci.* **2017**, *14*, 811.
[30] X. Guan, D. Lu, Z. Chen, Z. Wang, G. Zhou, Y. Fan, *Anal. Methods* **2023**, *15*, 3275.
[31] T. Peng, X. Liu, L. G. Adams, G. Agarwal, B. Akey, J. Cirillo, V. Deckert, S. Delfan, E. Fry, Z. Han, *Appl. Phys. Lett.* **2020**, *117*, 120601.
[32] Z. Wang, Z. Zheng, H. Hu, Q. Zhou, W. Liu, X. Li, Z. Liu, Y. Wang, Y. Ma, *Lab. Chip.* **2020**, *20*, 4255.
[33] Q. Bayin, L. Huang, C. Ren, Y. Fu, X. Ma, J. Guo, *Talanta* **2021**, *227*, 122207.
[34] FDA, In Vitro Diagnostics Emergency Use Authorizations (EUAs) - Serology and Other Adaptive Immune Response Tests for SARS-CoV-2), https://www.fda.gov/medical-devices/covid-19-emergency-use-authorizations-medical-devices/in-vitro-diagnostics-emergency-use-authorizations-euas-serology-and-other-adaptive-immune-response#individual-serological/, (accessed: March, 2023).
[35] Y. P. Hsu, N. S. Li, Y. T. Chen, H. H. Pang, K. C. Wei, H. W. Yang, *Biosens. Bioelectron.* **2020**, *151*, 111960.
[36] Y. P. Hsu, H. W. Yang, N. S. Li, Y. T. Chen, H. H. Pang, S. T. Pang, *ACS Sens.* **2020**, *5*, 928.
[37] T. Y. Lin, K. C. Wei, S. P. Ju, C. Y. Huang, H. W. Yang, *J. Mater. Chem. B* **2018**, *6*, 3387.
[38] W. Li, B. Chen, H. Zhang, Y. Sun, J. Wang, J. Zhang, Y. Fu, *Biosens. Bioelectron.* **2015**, *66*, 251.
[39] J. F. Masson, *ACS Sens.* **2020**, *5*, 3290.